JOURNAL OF CATALYSIS **87**, 116–125 (1984)

Optimal Catalyst Design for Ethylene Oxide Synthesis

M. MORBIDELLI, A. SERVIDA, R. PALUDETTO, AND S. CARRÀ

Dipartimento di Chimica Fisica Applicata, Politecnico di Milano, Piazza Leonardo da Vinci, 32, 20133 Milano, Italy

Received August 2, 1983; revised November 17, 1983

The performance of catalyst particles where parallel reactions take place can be significantly improved through the use of nonuniform activity distributions. The effectiveness factor and the global selectivity are the usual parameters used to judge on the particle performance. However, depending on the characteristics of the process considered, other integral parameters (combination of the previous two) can be more conveniently used to this purpose. With reference to the synthesis reaction of ethylene oxide, the most suitable objective function has been proposed and a very easy optimization technique, which identify a close approximation of the optimal radial activity distribution, has been developed. This leads to a Dirac delta function, in practice approximated by a step distribution whose width is about 4% of the particle radius, centered at a particular radial location within the particle, which depends on the operating conditions. Such activity distribution, which can be realized in practice with known impregnation techniques, leads to particle performances superior to the uniform one and to any nonuniform distribution previously proposed in the literature. Finally, the developed procedure can be successfully applied to other cases where two parallel reactions, with any kinetic expression, take place under nonisothermal conditions.

INTRODUCTION

It is well known that intraparticle mass and heat diffusion resistances largely affect the performance of a catalyst particle. This allows, in the case of supported catalyst particles, to identify suitable nonuniform distributions of the active catalyst within the inert support which significantly improve the particle performance. This can be realized in terms of the particle efficiency, selectivity (when competitive reactions are present), or, in the case of deactivating systems, in terms of the particle durability. Various analyses appeared in the literature devoted either to the theoretical definition of suitable activity distributions for some specific reacting systems, or to the experimental achievement of activity distributions of various shapes ((*1, 2*) and references therein).

In the following, the industrially relevant case of the ethylene oxide synthesis will be examined in detail.

Recently, Johnson and Verykios (*1*) have shown that the performance of this process can be significantly improved using activity distributions of the power law form.

The aim of this work is to define the optimal activity distribution which, for a given set of operating conditions, optimizes the particle performance. Such a distribution will be defined using the same optimization technique which has been successfully applied for the optimization of the catalyst particle effectiveness factor in the case of an isothermal Langmuir–Hinshelwood kinetics (*2, 3*).

According to (*1*), the following kinetic scheme proposed by Klugherz and Harriot (*4*) has been adopted

$$C_2H_4 + \tfrac{1}{2}O_2 \xrightarrow{1} C_2H_4O \qquad (1)$$

$$C_2H_4 + 3O_2 \xrightarrow{2} 2CO_2 + 2H_2O \qquad (2)$$

where the combustion reaction of ethylene oxide is neglected, due to its limited importance with respect to direct combustion of ethylene. The reaction rate expressions are, according to (*4*):

$$r_1 = k_1C_1C_2^2/F_1^2 \qquad (3)$$

0021-9517/84 $3.00

$$r_2 = k_2 C_1 C_2^2 / F_2^2 \quad (4)$$

where

$$F_1 = (0.0106 + 2144\, C_1 + 805\, C_2)(1 + 1271 \sqrt{C_2}) \quad (5)$$

$$F_2 = (0.008 + 4166\, C_1 + 1578\, C_2)(1 + 718 \sqrt{C_2}) \quad (6)$$

$$k_1 = k_1^0 \exp[\gamma_1(\theta - 1)/\theta] \quad (7)$$

$$k_2 = k_2^0 \exp[\gamma_2(\theta - 1)/\theta] \quad (8)$$

The reaction rate constants, k_1^0 and k_2^0, are evaluated at the temperature value of the catalyst particle surface, T^0. This has been assumed as $T^0 = 220°\mathrm{C}$, which is representative of industrial process temperatures, and corresponds to the value adopted by Klugherz and Harriot (*4*) in their experimental work. The dimensionless activation energies γ_1 and γ_2 have been estimated according to the values reported by Verykios *et al.* (*5*).

All the used kinetic data have been summarized in Table 1.

It is worthwhile to point out that the optimization technique which will be developed later, with reference to the case of ethylene oxide synthesis, can be easily extended to most parallel kinetic schemes operating under nonisothermal conditions.

THE OPTIMIZATION PROBLEM

The dimensionless mass and heat balances in a nonuniform catalyst particle, with negligible external resistances to mass and heat transfer, can be written as

$$L[u_1] = (\phi_1^2 f_1 + \phi_2^2 f_2) a(x) \quad (9)$$

$$L[u_2] = (\xi_1 \phi_1^2 f_1 + \xi_2 \phi_2^2 f_2) a(x) \quad (10)$$

$$L[\theta] = -(\beta_1 \phi_1^2 f_1 + \beta_2 \phi_2^2 f_2) a(x) \quad (11)$$

with boundary conditions (BCs)

$$u_1 = u_2 = \theta = 1 \qquad \text{at } x = 1 \quad (12a)$$

$$\frac{du_1}{dx} = \frac{du_2}{dx} = \frac{d\theta}{dx} = 0 \qquad \text{at } x = 0 \quad (12b)$$

where the following dimensionless quantities have been used

$$\theta = T/T^0 \qquad u_1 = C_1/C_1^0 \qquad u_2 = C_2/C_2^0 \qquad x = r_p/R_p$$

$$\phi_1^2 = \frac{R_p^2}{D_1 C_1^0} r_1^0 \qquad \phi_2^2 = \frac{R_p^2}{D_1 C_1^0} r_2^0 \qquad \xi = \frac{C_1^0 D_1}{C_2^0 D_2}$$

$$\xi_1 = \tfrac{1}{2}\xi \qquad \xi_2 = 3\xi$$

$$\beta_1 = \frac{(-\Delta H_1) D_1 C_1^0}{\lambda T^0} \qquad \beta_2 = \frac{(-\Delta H_2) D_1 C_1^0}{\lambda T^0} \qquad \rho(\theta) = \frac{\theta - 1}{\theta} \quad (13)$$

$$f_1 = \frac{r_1}{r_1^0} = \frac{u_1 u_2^2 F_1^{0^2} \exp(\gamma_1 \rho(\theta))}{F_1^2} \qquad f_2 = \frac{r_2}{r_2^0} = \frac{u_1 u_2^2 F_2^{0^2} \exp(\gamma_2 \rho(\theta))}{F_2^2}$$

and the operator $L[\ ]$ is defined as

$$L[\ ] = \frac{1}{x^n} \frac{d}{dx}\left(x^n \frac{d[\ ]}{dx}\right) \quad (14)$$

where the integer $n = 0, 1, 2$ indicates the infinite slab, infinite cylinder and sphere, respectively.

The reaction rate expressions r_1^0 and r_2^0, which appear in the definition of the Thiele modulus, are evaluated at the particle surface conditions, i.e., $r_1^0 = \bar{k}_1^0 C_1^0 C_2^{0^2} / F_1^{0^2}$; $\bar{k}_1^0$ is the volume average reaction rate constant defined as

$$\bar{k}_1^0 = \frac{1}{V_p} \int_{V_p} k_1^0(r_p)\, dV_p \quad (15)$$

where $k_1^0(r_p)$ is the local value, which depends on the local concentration of active

TABLE 1

Parameter Values Used in the Reported Calculations

$C_1^0 = 1.24\ 10^{-6}$ mole/cm^3	$\Delta H_1 = -28670$ cal/mole
$C_2^0 = 3.72\ 10^{-6}$ mole/cm^3	$\Delta H_2 = -316300$ cal/mole
$T^0 = 493$ K	$\phi_2^2 = 1.16\ \phi_1^2$
$n = 2$	$\beta_2 = 11\beta_1$
$k_1^0 = 8.63\ 10^6$ mole/s cm^3	$\xi_1 = 0.1315$
$k_2^0 = 6.57\ 10^6$ mole/s cm^3	$\xi_2 = 0.789$
$\gamma_1 = 21.9$	$\xi = 0.263$
$\gamma_2 = 29.7$	$\bar{c} = 10$

catalyst. The activity distribution is usually defined as $a(r_p) = k_1^0(r_p)/\bar{k}_1^0$ (or $a(r_p) = k_2^0(r_p)/\bar{k}_2^0$, which is obviously identical), and thus it must satisfy the integral condition derived from Eq. (15), which, in dimensionless variables, can be written as

$$(n + 1) \int_0^1 a(x)x^n dx = 1 \qquad (16)$$

Note that the total amount of active catalyst appears only in the expression of the volume average reaction rate constant, which will be then kept constant while comparing various expressions of $a(x)$ in order to guarantee equal total amount of active catalyst.

The solution of the system of differential Equations (9)–(12) can be facilitated through the introduction of the following invariant

$$L[(\beta_2\xi_1 - \beta_1\xi_2)u_1 + (\beta_1 - \beta_2)u_2 - (\xi_2 - \xi_1)\theta] = 0 \qquad (17)$$

which integrated with the boundary conditions (12) leads to

$$(\xi_1\beta_2 - \xi_2\beta_1)u_1 + (\beta_1 - \beta_2)u_2 - (\xi_2 - \xi_1)\theta + (\xi_2 - \xi_1 - \beta_1 + \beta_2 - \xi_1\beta_2 + \xi_2\beta_1) = 0 \qquad (18)$$

This constitutes a linear relationship between the three unknowns, which can obviously replace one of the differential Equations (9)–(11). It is worthwhile to point out that this is the only invariant present in the problem and then at least two differential equations must be integrated simultaneously.

It is now necessary to introduce a significant objective function for the optimization problem under examination. Three quantities can be considered, each indicative of one particular aspect of the particle performance. The effectiveness factor

$$\eta = \frac{(n + 1)}{(\phi_1^2 + \phi_2^2)} \int_0^1 (\phi_1^2 f_1 + \phi_2^2 f_2) a(x)x^n dx \qquad (19)$$

which indicates the ratio between the actual total ethylene consumption rate and the same quantity evaluated at the particle external surface conditions. The global normalized selectivity, S, defined as the ratio between the actual global selectivity, s, given by

$$s = \frac{\int_0^1 \phi_1^2 f_1 a(x)x^n dx}{\int_0^1 (\phi_1^2 f_1 + \phi_2^2 f_2) a(x)x^n dx} \qquad (20)$$

and the global selectivity evaluated at the surface conditions, s^0:

$$S = \frac{s}{s^0} = \frac{(\phi_1^2 + \phi_2^2) \int_0^1 f_1 a(x)x^n dx}{\int_0^1 (\phi_1^2 f_1 + \phi_2^2 f_2) a(x)x^n dx} \qquad (21)$$

which represents the amount of ethylene oxide produced per unit of ethylene consumed. Finally, the overall normalized rate of ethylene oxide production, R, can be defined as

$$R = \eta S \qquad (22)$$

which obviously indicates the absolute amount of ethylene oxide produced.

Each of these parameters considers one important aspect of the process efficiency, but cannot be used as the global objective function. In fact, in industrial reactors the outlet per pass conversion is held to about 30% in order to maintain high selectivity values, and the exit stream, after removal of ethylene oxide and carbon dioxide, is recycled back to the reactor (*6*). Therefore, the economy of the process requires high selectivity, in order to reduce the ethylene amount wasted by the complete combustion reaction, and large per pass conversion in order to reduce the recycle cost. An accurate optimization of the process would obviously require the modeling of the entire reactor, including the combustion reaction of ethylene oxide which can be significant at large ethylene conversion. This is clearly beyond the scope of this work, but it shows that in the optimization of the particle performance both selectivity and effectiveness factor must be taken into account. In particular, for a given ethylene feed flow rate, the profit of the process is proportional to the sum of two contributions: one due to the value of ethylene oxide produced and the other one to ethylene conversion, which allows saving of the recycle cost:

$$P = \eta(1 + \bar{c}s)/(1 + \bar{c}s^0) \qquad (23)$$

where $\bar{c}$ indicates the ratio between the cost of 1 mole of ethylene oxide and the recycle cost per mole of recycled ethylene, and the denominator has been added in order to normalize the variable P with respect to its value at the particle external surface conditions.

The optimization problem is now fully defined: we want to determine the activity distribution function $a(x)$, which maximizes the objective function P under the constraint given by Eq. (16):

$$\max_{a(x)} P(a(x),u_1(x),u_2(x),\theta(x)) \qquad (24)$$

where u_1, u_2, and θ are given by the system of differential Eqs. (9)–(12). It is worthwhile to point out that the same problem can be applied to the other integral parameters characteristic of the particle performance: effectiveness factor, selectivity, and overall production rate. The optimization technique will be described in detail only for the case of the profit objective function, P, since its extension to the others is straightforward.

OPTIMAL ACTIVITY DISTRIBUTION

The optimization problem can be solved using the same technique developed by Morbidelli *et al.* (*2*) in the case of an isothermal Langmuir–Hinshelwood kinetics. To this aim it is convenient to rewrite the objective function (23) in the form

$$P = \int_0^1 g(u_1,u_2,\theta)a(x)x^n dx \qquad (25)$$

where

$$g(u_1,u_2,\theta) = (n + 1)[(1 + \bar{c})\phi_1^2 f_1 + \phi_2^2 f_2]/[(1 + \bar{c})\phi_1^2 + \phi_2^2] \qquad (26)$$

Introducing the local selectivity

$$s_l = \frac{\phi_1^2 f_1}{\phi_1^2 f_1 + \phi_2^2 f_2} \qquad (27)$$

and combining Eqs. (9) and (10), it can be obtained

$$L[u_2] = [\xi_2 + s_l(\xi_1 - \xi_2)]L[u_1] \qquad (28)$$

which can be integrated using the BCs (12b) and assuming that

$$[\xi_2 + s_l(\xi_1 - \xi_2)] = \text{const} \qquad (29)$$

leading to

$$du_2 = [\xi_2 + s_l(\xi_1 - \xi_2)]du_1 \qquad (30)$$

This approximate relationship has been used by Johnson and Verykios (*1*) in their numerical procedure for the solution of the particle mass balances. Its accuracy is obviously dependent on the accuracy of assumption (29), which should be reasonable in the range of parameter values of practical interest (see in particular ξ_1 and ξ_2 in Table 1). Moreover, from Eq. (27) it appears that the local selectivity depends solely on the ratio $(f_2/f_1) = (F_1/F_2)^2(F_2^0/F_1^0)^2\exp[(\gamma_2 - \gamma_1)\rho(\theta)]$, which is a weak function of temperature and composition. Substituting the expression for θ given by Eq. (18), and integrating Eq. (30), with the initial condition $u_2 = 1$ at $u_1 = 1$, an explicit expression of u_2 as a function of u_1 can be derived. Such relationship, together with Eq. (18) for θ, allows to represent the function defined by Eq. (26) in terms of the only variable u_1, i.e., $g(u_1,u_2,\theta) = h(u_1)$. Note that for our purposes it is sufficient to prove the existence of the function $h(u_1)$, even though it can not be derived analytically.

Let us define $\bar{u}_1$, the value of u_1 which maximizes the function $h(u_1)$:

$$\max_{u_1} h(u_1) = g(\bar{u}_1,u_2(\bar{u}_1),\theta(\bar{u}_1)) = H \quad (31)$$

using Eq. (16), it follows that

$$P \leqq H/(n + 1) \quad (32)$$

So that, if there exists a distribution $a(x)$ such that $P = H/(n + 1)$, this would obviously be the optimal one. Such a distribution exists and is given by

$$a(x) = \delta(x - \bar{x})/(n + 1)\bar{x}^n \quad (33a)$$

where $\delta(x - \bar{x})$ is a Dirac delta function, and $\bar{x}$ is the dimensionless radial position where $u_1 = \bar{u}_1$, i.e.,

$$u_1 = \bar{u}_1 \text{ at } x = \bar{x} \quad (33b)$$

This can be easily verified by substituting Eqs. (33) in Eq. (25). The obtained solution can obviously be accepted only if Eq. (33b) is satisfied for $\bar{x} \in [0,1]$.

From a practical point of view, the activity distribution (33a) is obviously not feasible. However, it can be approximated by locating the active catalyst in a narrow region centered about the optimal location $x = \bar{x}$, using a limited total amount of catalyst in order to avoid metal dispersion problems. A sensitivity analysis performed by Morbidelli *et al.* (*2*) showed that locating the catalyst in a region of width equal to about 4% of the particle radius, it is possible to closely approximate the performance of a catalyst particle with a Dirac activity distribution function.

It is worthwhile to point out that the optimal activity distribution (33a) has been derived using the approximate relationship (30), so that it can not be considered as the rigorous optimum. However, since in the case under examination Eq. (30) is rather accurate, it can be expected that the activity distribution (33a) would lead to excellent particle performances, particularly with respect to other distributions previously proposed in the literature.

In order now to define the optimal location $\bar{x}$ as a function of the various involved parameters, it is convenient to first solve Eqs. (9)–(12) with the activity distribution (33), and then to identify the $\bar{x}$ value which maximizes the considered objective function. The integration of the particle mass balances (9) and (10), using the activity distribution (33a), can be easily performed in the two subintervals of the integration domain, $x \in [0,\bar{x}]$ and $x \in [\bar{x},1]$, using the BCs (12a) and (12b), respectively, as

$$u_1 = \bar{u}_1 \quad ; \quad u_2 = \bar{u}_2 \qquad \text{for } x \in [0,\bar{x}] \quad (34a)$$

$$u_1 = 1 + A\Psi_n(x) \quad ; \quad u_2 = 1 + B\Psi_n(x) \qquad \text{for } x \in [\bar{x},1] \quad (34b)$$

where

$$\Psi_n(x) = \begin{cases} x - 1 & \text{for } n = 0 \\ \ln x & \text{for } n = 1 \\ 1 - \dfrac{1}{x} & \text{for } n = 2 \end{cases} \quad (34c)$$

and $\bar{u}_1$, $\bar{u}_2$, A, and B are integration constants which can be readily derived through the continuity conditions at $x = \bar{x}$:

$$\bar{u}_1 = 1 + A\Psi_n(\bar{x})$$

$$\bar{u}_2 = 1 + B\Psi_n(\bar{x}) \quad (35)$$

and the global conditions obtained by equating the concentration gradient evaluated at $x = 1$ estimated using both Eq. (34b) and the mass balances (9) and (10)

$$\left(\frac{du_1}{dx}\right)_{x=1} = A = \frac{1}{(n + 1)} (\phi_1^2\bar{f}_1 + \phi_2^2\bar{f}_2) \quad (36a)$$

$$\left(\frac{du_2}{dx}\right)_{x=1} = B = \frac{1}{(n + 1)} (\xi_1\phi_1^2\bar{f}_1 + \xi_2\phi_2^2\bar{f}_2) \quad (36b)$$

where the superscript $^-$ indicates a quantity evaluated at $x = \bar{x}$. The values of $\bar{u}_1$ and $\bar{u}_2$

can be calculated from the system of algebraic equations, derived by substituting Eqs. (36) in Eqs. (35):

$$\bar{u}_1 = 1 + \frac{\Psi_n(\bar{x})}{(n+1)}(\phi_1^2\bar{f}_1 + \phi_2^2\bar{f}_2) \quad (37a)$$

$$\bar{u}_2 = 1 + \frac{\Psi_n(\bar{x})}{(n+1)}(\xi_1\phi_1^2\bar{f}_1 + \xi_2\phi_2^2\bar{f}_2) \quad (37b)$$

while $\bar{\theta}$ readily derives from Eq. (18). The expressions for the evaluation of the integral characteristic parameters of the particle performance: η, S, R, and P, are readily derived from their definitions and have been summarized in Table 2. The search of the optimal location $\bar{x}$ can then be performed numerically as described in detail in the next section.

RESULTS AND DISCUSSION

The system of Eqs. (37a), (37b), and (18), for a given values of ϕ_1^2, $\bar{x}$ and the other involved parameters, using $\bar{u}_1$, $\bar{u}_2$, and $\bar{\theta}$ as unknowns can exhibit multiple solutions, and consequently convergence difficulties. This can be avoided, as usual in problems of this type, formulating the problem in a different form, which exhibits a unique solution: $\bar{x}$ and $\bar{u}_1$ are given as input data, while $\bar{u}_2$, $\bar{\theta}$, and ϕ_1^2 are unknown. Moreover, by combining Eqs. (37a) and (37b) it can be seen that

$$\frac{\bar{u}_1 - 1}{\bar{u}_2 - 1} = \frac{(\phi_1^2\bar{f}_1 + \phi_2^2\bar{f}_2)}{(\xi_1\phi_1^2\bar{f}_1 + \xi_2\phi_2^2\bar{f}_2)} \quad (38)$$

where, since from Eq. (13) it follows that the ratio $\phi_1^2/\phi_2^2 = r_1^0/r_2^0$ is a constant value dependent only on the conditions at the external particle surface, the r.h.s. is independent of $\bar{x}$ and ϕ_1^2.

Therefore, the values $\bar{u}_2$ and $\bar{\theta}$ (which can be derived from Eqs. (38) and (18)) assume, for a given $\bar{u}_1$, the same value for all values of the catalyst location, $\bar{x}$. Since the same situation occurs for the integral characteristic parameters reported in Table 2, it can be concluded that also this quantities are independent of the catalyst location $\bar{x}$. Using the parameter values summarized in Table 1, which are representative of usual industrial operating conditions (*1*), the values of the parameters η, S, R, and P can be calculated as a function of $\bar{u}_1$, for all possible values of the catalyst location $\bar{x}$, as shown in Fig. 1a. On the other hand, once $\bar{u}_2$ and $\bar{\theta}$ are evaluated, the Thiele modulus ϕ_1^2 can be calculated, as a function of $\bar{x}$, using Eq. (37a). The obtained values of ϕ_1^2 as a function of $\bar{u}_1$, for various values of $\bar{x}$, are shown in Fig. 1b. It is remarkable that, for a given $\bar{u}_1$ value, from Eq. (37a) it appears that

$$\phi_1^2(\bar{x}) = \phi_1^2(\bar{x}_0)\frac{\Psi_n(\bar{x}_0)}{\Psi_n(\bar{x})} \quad (39)$$

which allows, once the ϕ_1^2 vs $\bar{u}_1$ has been calculated for one value of the optimal location $\bar{x} = \bar{x}_0$, to readily compute the same curve for any other given value of $\bar{x}$. So, the construction of the curves shown in Figs. 1a and b, actually requires the numerical solution of only one problem with fixed $\bar{x}$. These figures summarize all the informations necessary to define the optimal catalyst location. In particular, from Fig. 1a the value of $\bar{u}_1$ which maximizes the desired characteristic parameter is determined, and then the value of $\bar{x}$ which allows to realize the so determined $\bar{u}_1$ is estimated, for a given value of ϕ_1^2, from Fig. 1b. As expected, it can be seen that the optimal catalyst location changes depending on which integral characteristic parameter is to be maximized. In particular, the global selectivity reaches its maximum value at the particle surface, as it is expected for exother-

TABLE 2

Expressions of the Integral Characteristic Parameters of a Catalyst Particle with the Activity Distribution (33a)

$\eta = \dfrac{\phi_1^2\bar{f}_1 + \phi_2^2\bar{f}_2}{\phi_1^2 + \phi_2^2}$	$S = \dfrac{(\phi_1^2 + \phi_2^2)\bar{f}_1}{\phi_1^2\bar{f}_1 + \phi_2^2\bar{f}_2}$
$R = \bar{f}_1$	$P = \dfrac{\phi_1^2(1+\bar{c})\bar{f}_1 + \phi_2^2\bar{f}_2}{\phi_1^2(1+\bar{c}) + \phi_2^2}$

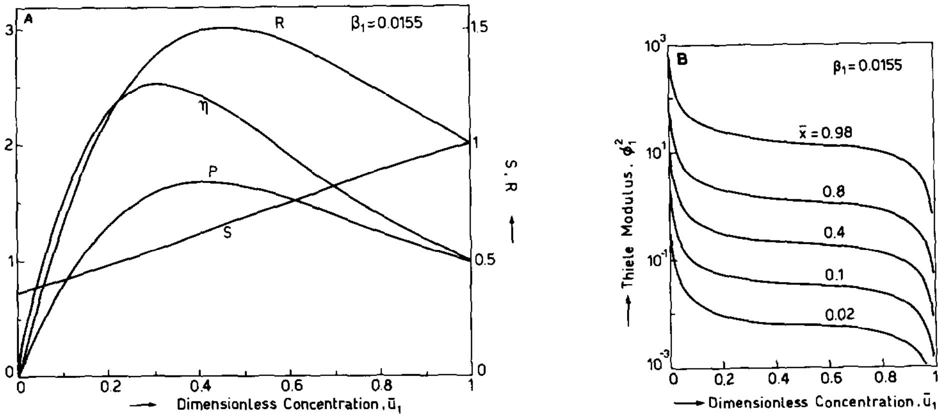

FIG. 1. (a) Integral characteristic parameters as a function of the dimensionless concentration value $\bar{u}_1$ for a nonuniform catalyst particle with activity distribution (33); $\beta_1 = 0.0155$. (b) Relationship between the values of $\bar{u}_1$, reported in Fig. 1a, and the Thiele Modulus ϕ_1^2.

mic parallel reactions, when the desired reaction has the lowest activation energy. The same data are shown in Figs. 2a and b for increased values of the heat of reaction parameters β_1 and β_2. This case exhibits the usual multiplicity behavior characteristic of nonisothermal catalyst particles. Thus, the steady states characterized by a positive slope of the ϕ_1^2 vs $\bar{u}_1$ curve are unstable, and then not attainable by the system, and the local maximum and minimum values of ϕ_1 indicate the bifurcation points.

Note that in both Figs. 1b and 2b the examined values of the active catalyst location range in the interval $\bar{x} \in [0.02, 0.98]$, since in practice the activity distribution (33a) is replaced by a step distribution centered about $\bar{x}$ and with dimensionless width equal to 0.04. Moreover, although not indicated in the figures, it readily follows from Eq. (37a) that the asymptotic behavior of each ϕ_1^2 vs $\bar{u}_1$ curve, at fixed $\bar{x}$, is $\phi_1^2 \to \infty$ at $\bar{u}_1 \to 0$ and $\phi_1^2 \to 0$ at $\bar{u} \to 1$.

From inspection of Figs. 1b and 2b it appears that for very large or low Thiele modulus values, the value of $\bar{x} \in [0.02, 0.98]$ which realizes a desired $\bar{u}_1$ value may not exist. In fact, in order to obtain a given $\bar{u}_1$ value for $\phi_1 \to \infty$ ($\phi_1 \to 0$), the optimal catalyst location $\bar{x} \to 1$ ($\bar{x} \to 0$) as it can be seen

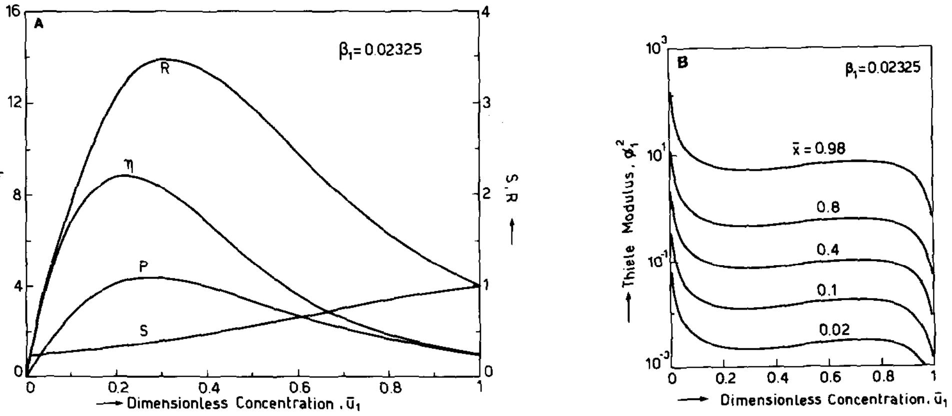

FIG. 2. (a) Integral characteristic parameters as a function of the dimensionless concentration value $\bar{u}_1$ for a nonuniform catalyst particle with activity distribution (33); $\beta_1 = 0.02325$. (b) Relationship between the values of $\bar{u}_1$, reported in Fig. 2a, and the Thiele Modulus ϕ_1^2.

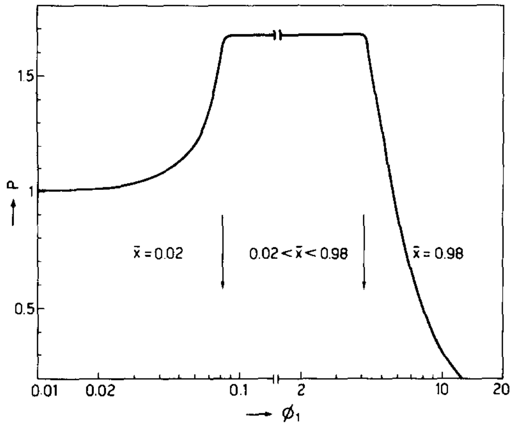

FIG. 3. Optimal value of the normalized process profit parameter P as a function of the Thiele Modulus ϕ_1.

from Eqs. (37a) and (34c). The plane geometry exhibits an irregular behavior for $\phi_1 \rightarrow 0$, leading to negative values of $\bar{x}$, which for physical reasons should be replaced by $\bar{x} = 0$ (as in the case of Laugmuir–Hinshelwood kinetics (*2*, *3*)). Thus, in practice, for very large (small) values of the Thiele modulus, the active catalyst should be located at $\bar{x} = 0.98$ ($\bar{x} = 0.02$). In conclusion, the values of the objective function P obtained as a function of the Thiele modulus ϕ_1 using the optimal catalyst activity distribution (33) are shown in Fig. 3. The optimal location $\bar{x}$ depends on the value of the Thiele modulus for $0.083 < \phi_1 < 4.1$, and can be calculated from the curves shown in Figs. 1a and b, while for larger or smaller ϕ_1 value is $\bar{x} = 0.98$ or 0.02, respectively.

With illustrative purposes the same calculations have been performed using the activity distribution proposed by Johnson and Verykios (*1*)

$$a(x) = \frac{\alpha + n + 1}{n + 1} x^{\alpha} \tag{40}$$

with $\alpha = 0$ (corresponding to a uniformly impregnated particle), 3, 6, and 9. The values of the integral characteristic parameters obtained for each of such distributions are shown in Figs. 4 to 7. The differences between the results here shown and those reported by Johnson and Verykios (*1*) are due to some possible differences in the kinetic rate constant values (not reported in detail in that work) and to the use of the approximate Eq. (30) instead of the oxygen mass balance (10). The calculation reported in Figs. 4 to 7 have been obtained through numerical integration of the exact system of equations (i.e., Eqs. (9), (10), and (18)), using the orthogonal collocation method on finite elements (*7*, *8*). The use of finite elements is required by the steepness of the concentration profiles within the particle caused by both the steepness of the activity profile (particularly at large values of the parameter α) and the magnitude of the Thiele modulus value. Two elements were

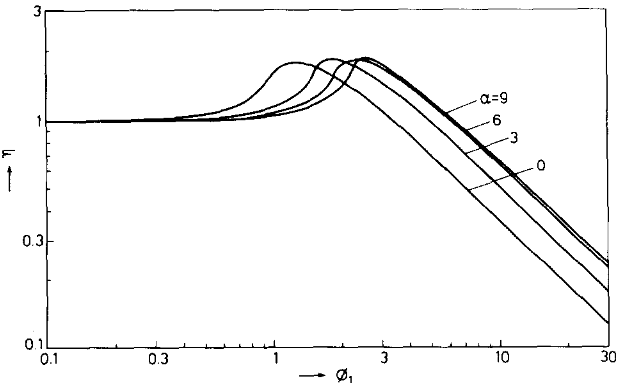

FIG. 4. Effectiveness factor η vs Thiele Modulus ϕ_1, for a nonuniform catalyst particle with activity distribution (40).

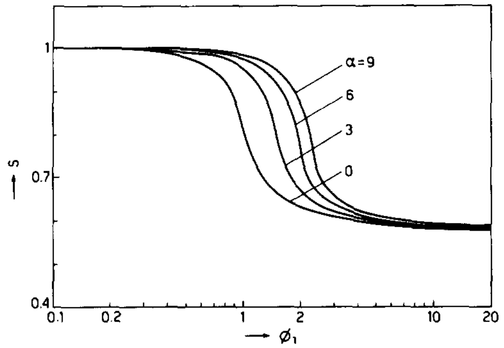

FIG. 5. Global normalized selectivity S vs Thiele Modulus ϕ_1, for a nonuniform catalyst particle with activity distribution (40).

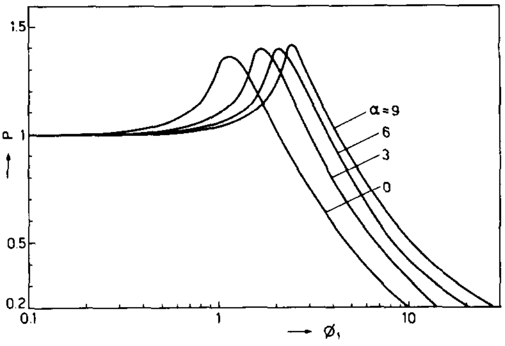

FIG. 7. Normalized process profit parameter P vs Thiele Modulus ϕ_1 for a nonuniform catalyst particle with activity distribution (40).

used for $\phi_1^2 < 10$, locating the boundary between the two elements at the coordinate value where the activity is about equal to 10^{-3}, so that in the inner element of the pellet almost no reaction is taking place. Usually, four collocation points are necessary in this element, and ten in the outer one. For larger values of the Thiele modulus, $\phi_1^2 > 10$, the outer element has been further divided in two elements, locating the boundary at a distance from the particle surface of the order of $1/\phi_1\sqrt{a}(1)$. In each of such elements about seven collocation points were introduced. The standard technique of the orthogonal collocation method (*7*, *8*) using the Jacoby polynomials $P_i^{(\alpha,\beta)}(x)$ as trial functions with $\alpha = \beta = 0$, has then been applied.

Using Figs. 3 and 7, it is possible to compare the values of the characteristic parameter P, significative of the normalized process profit, obtained using the activity distribution (40) and the optimal one previously determined. It is apparent that the optimal activity distribution leads to larger P values for all the Thiele modulus values. The only exception is the region of large ϕ_1 values, where the optimization procedure would lead to a Dirac activity distribution closer to the particle surface than $\bar{x} = 0.98$. Since we have imposed $\bar{x} < 0.98$, it follows that, in this region, activity distributions other than the Dirac one, such as that given by Eq. (40), can lead to better performances of the catalyst particle. It is noticeable that for the industrial ethylene oxide synthesis (*1*) is $\phi_1 \simeq 1.4$. In this case, as previously pointed out by Johnson and Verykios (*1*), the uniform activity distribution and the one given by Eq. (40) with $\alpha = 3$, give the same overall rate of ethylene oxide formation (i.e., $R \simeq 1.2$), but the second one leads to a selectivity increase of about 26.9%, as it appears in Figs. 5 and 6. From Fig. 1 it can be seen that the optimal distribution, operating with the same R value, leads to a selectivity increase, with respect to the uniform one, of about 34.3%, and is obtained by locating the active catalyst at $\bar{x} = 0.82$. Therefore, the optimal activity distribution (33) can significantly improve the catalyst particle performance. This has been represented in this work by the process profit parameter P; however, the same

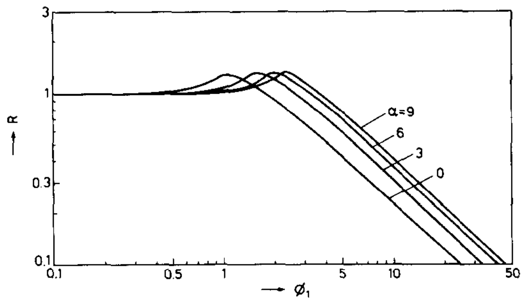

FIG. 6. Overall normalized production rate of ethylene oxide R vs Thiele Modulus ϕ_1, for a nonuniform catalyst particle with activity distribution (40).

optimization procedure can be immediately applied to other integral parameters characteristic of the particle performance. Finally, note that the outlined procedure is of general validity for parallel reaction schemes with any reaction kinetics, and the obtained results apply qualitatively to any case where the activation energy of the desired reaction is lower than that of the undesired one.

APPENDIX: NOMENCLATURE

a	activity distribution function
$\bar{c}$	ratio between the cost of 1 mole of ethylene oxide and the recycle cost per unit of recycled ethylene
C_i	concentration of the ith component
D	effective diffusion coefficient
E_j	activation energy
f_j	r_j/r_j^0
F_j	functions defined by Eqs. (5) and (6)
g	function defined by Eq. (26)
H	parameter defined by Eq. (31)
$k_j,\bar{k}_j$	local and volume average reaction rate constants
$L[\ ]$	differential operator defined by Eq. (14)
n	integer characteristic of pellet geometry; $n = 0$ for infinite slab; $n = 1$ for infinite cylinder; $n = 2$ for sphere
P	normalized process profit parameter, defined by Eq. (23)
r_j	rate of the jth reaction
r_p	distance from the center of the pellet
R	overall normalized production of ethylene oxide, defined by Eq. (22)
R_p	characteristic pellet dimension; half thickness ($n = 0$), radius ($n = 1,2$)
s	global selectivity, defined by Eq. (20)
s_l	local selectivity, defined by Eq. (27)
S	global normalized selectivity, defined by Eq. (21)
T	temperature
u_i	C_i/C_i^0
V_p	pellet volume
x	r_p/R_p

Greek Letters

α	exponent of the power law activity distribution
β_j	$(-\Delta H_j)D_1C_1^0/\lambda T^0$
γ_j	E_j/RT^0
δ	Dirac delta function
ΔH_j	standard enthalpy change of the jth reaction
θ	T/T^0
γ	effective thermal conductivity of catalyst particle
ξ	$C_1^0D_1/C_2^0D_2$
ξ_j	defined by Eq. (13)
ρ	$(\theta - 1)/\theta$
ϕ_j	Thiele modulus
Ψ_n	function defined by Eq. (34c)

Subscripts

i	component
j	reaction
1	ethylene or reaction (1)
2	oxygen or reaction (2)

Superscripts

^{0}	external particle surface
$\bar{\ }$	location of the active catalyst

REFERENCES

1. Johnson, D. L., and Verykios, X. E., *J. Catal.* **79,** 156 (1983).
2. Morbidelli, M., Servida, A., and Varma, A., *Ind. Eng. Chem. Fundam.* **21,** 278 (1982).
3. Morbidelli, M., and Varma, A., *Ind. Eng. Chem. Fundam.* **21,** 284 (1982).
4. Klugherz, P. D., and Harriot, P., *AIChE J.* **17,** 856 (1971).
5. Verykios, X. E., Stein, F. P., and Coughlin, R. W., *Catal. Rev. Sci. Eng.* **22,** 197 (1980).
6. Zomerdijk, J. C., and Hall, M. W., *Catal. Rev. Sci. Eng.* **23,** 163 (1981).
7. Villadsen, J., and Michelsen, M. L., "Solution of Differential Equation Models by Polynomial Approximation." Prentice–Hall, Englewood Cliffs, N.J., 1978.
8. Finlayson, B. A., "The Method of Weighted Residuals and Variational Principles." Academic Press, New York, 1972.